EMAS Engineering Modelling, Analysis & Simulation THE NAFEMS JOURNAL

NAFEMS

Vol. 2, Issue 1, 2025

Nonlinear Dynamic Analysis Using Harmonic Balance Method

M. Klein[a,1], R. Helfrich[a], T. Willerding[a]

[a]INTES GmbH, Breitwiesenstrasse 28, 70565 Stuttgart, Germany

Abstract

There is a high demand for nonlinear structural dynamics in implicit Finite Element Analysis (FEA). Although such methods are available, there are several obstacles to use them daily. One is their extreme and unpredictable computation time, which makes it often impossible to get results in time. Another point is the restriction of the methods to the time domain, which is often in contrary to the usual design rules based on frequency domain results. The Harmonic Balance Method (HBM) is a solution for an important sub-class of analysis cases, which resolves the two mentioned obstacles. As a starting point, we define HBM as a frequency response analysis with local nonlinearities. This allows to solve contact problems or mounting problems with nonlinear force-deflection curves. The primary results of HBM are in frequency domain. For all calculated frequencies, a solution in time domain is also available for a periodic response. A simplified radiator is used as industrial example. To prove the validity of HBM, a comparison with a linear frequency response analysis is performed, which shows same results. Then, rubber bushes and contact are added to the model as nonlinearities. Key results of stress and fatigue are presented, and the computation times are analysed to demonstrate the feasibility of the HBM implementation for applications in research and industry. All simulations are performed with the FEA software PERMAS, which contains the HBM among many other analysis methods in structural dynamics.

Keywords

Harmonic Balance Method (HBM), local nonlinearities, frequency domain, time domain, nonlinear dynamics, stress analysis, fatigue analysis

1 Introduction

The theoretical basis of the HBM ([1]-[6])is an extension of the linear formulation as for a frequency response analysis by a nonlinear term:

$$\mathrm{M\ddot{u} + C\dot{u} + Ku + f_{nl}(\dot{u}, u) = f_{ext}(t)} \tag{1}$$

with time-periodic excitation

$$\mathrm{f_{ext}(t) = f_{ext}(t+T), T = \frac{2\pi}{\omega}}. \tag{2}$$

Typically, a truncated Fourier series is used for the excitation

$$f_{ext}(t) \approx f_0 + \sum_{k=1}^{r} (f_c^k \cos k\,\omega t + f_s^k \sin k\,\omega t) \tag{3}$$

and for the displacement result:

[1]Corresponding author.

E-mail address: klein@intes.de (M. Klein)

https://doi.org/10.59972/thsz7utp

$$u(t) \approx u_0 + \sum_{k=1}^{r} (u_c^k \cos k\,\omega t + u_s^k \sin k\,\omega t) \tag{4}$$

In FEA, the nonlinear term in (1) is modelled by nonlinear elements like nonlinear spring elements for the stiffness, where the force-deflection relationship is nonlinear. Where necessary, the damping can be modelled by nonlinear damping elements as well.

2 Example Model

The following example of a simple radiator in Figure 1 is used to demonstrate the use of the HBM. The dynamic loading is a sine function using the self-weight in Z direction. The model has about 400k nodes and 750k solid elements. In order to compare results for the same node, a reference node has been selected as depicted in Figure 2. The mounting of the radiator has two components for each of the four pins. One component is a rubber mount, and the other component is the contact between the pin and the rubber. A first analysis will show the effect of the rubber, and a second analysis will show the results of both rubber and contact. The shape of the rubber mounts and the position of the rubber mounts is shown in Figure 3 and Figure 4. Due to a different shape in XY plane compared to XZ and YZ plane, we have different force-deflection characteristics of the rubber mount in XY plane (see Figure 4) compared to Z direction (see Figure 5). The characteristics were found by a nonlinear analysis using a reduced polynomial strain energy potential for the rubber. Of course, test results of the force-deflection characteristics could also be used. Then, a fitting is used to find nonlinear polynomials for the force deflection curves. These polynomials are used to define the behaviour of nonlinear spring elements.

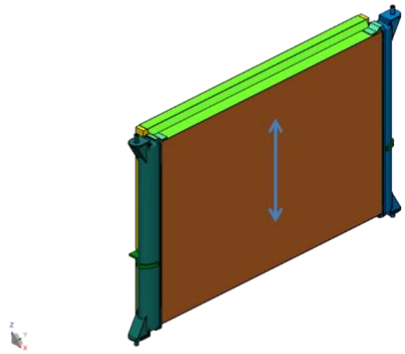

Figure 1. Example of a radiator.

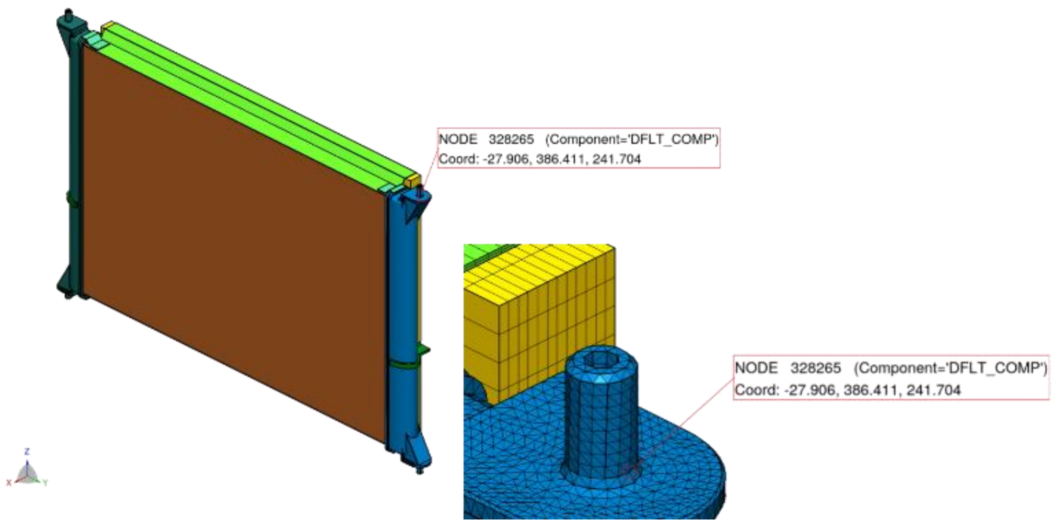

Figure 2. The node 328265 is used as reference node to compare the results at the right upper mounting pin of the radiator.

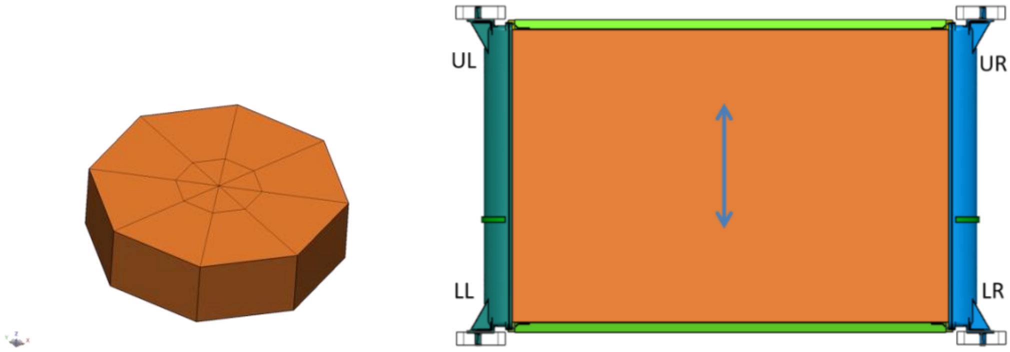

Figure 3. The rubber mounts have a circular shape in XY plain and are like a plate in Z direction. The rubber mounts are applied at the upper left (UL), upper right (UR), lower left (LL), and lower right (LR) pin of the radiator.

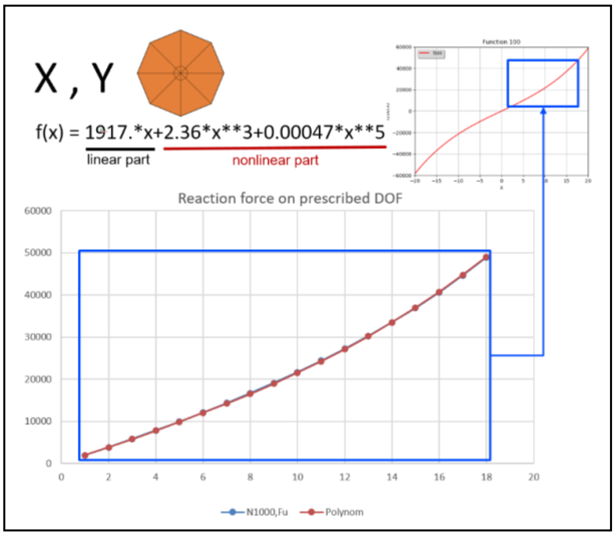

Figure 4. The calculated rubber mount force-deflection [N – mm] curve in XY plane with the fitted polynomial of 5th order.

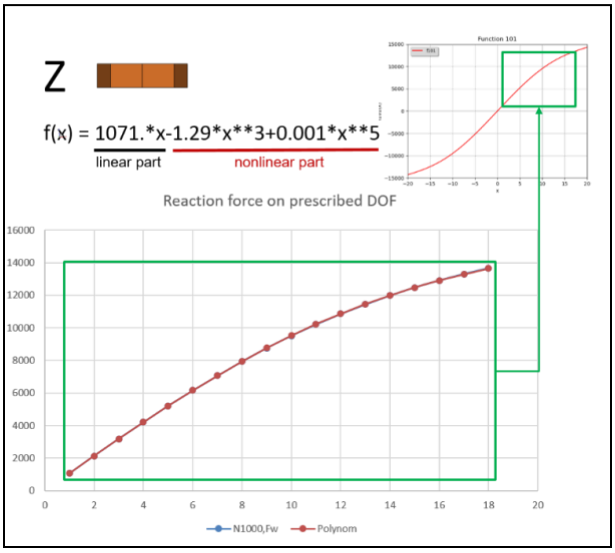

Figure 5. The calculated rubber mount force-deflection [N – mm] curve in Z direction with the fitted polynomial of 5th order.

3 First Analysis: Rubber Mounts Only

Our first study will be made with the rubber mounts only neglecting the effect of contact between pin and rubber mount. Figure 6 shows the modeling of one spring-damper system, which represents a rubber mount. This system has to be duplicated for all directions at all four pins. The two end-nodes of the spring-damper system have the same position in space. One is connected to a center node of the pin, while the other is fixed.

The force-deflection curves of the nonlinear spring are taken from Figure 4 and Figure 5 respectively. Such spring-damper systems must be created for all directions at all four mounting pins. While the springs behave nonlinearly, we decided to use a linear function for all dampers to make it easier for the reader to understand the results.

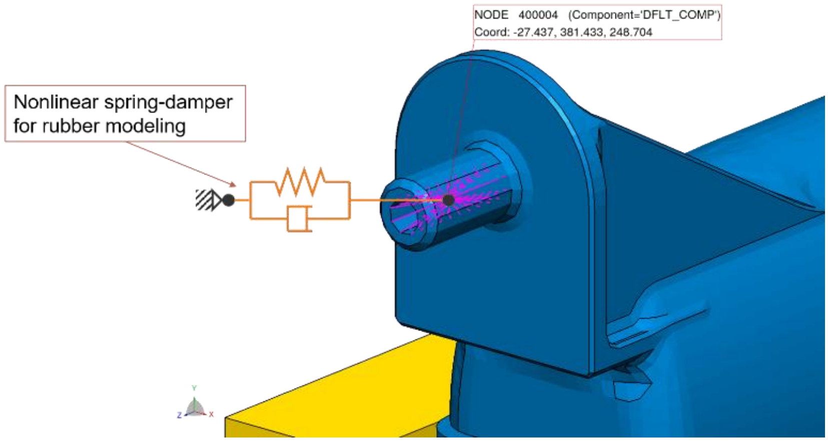

Figure 6. The modeling of a rubber mount by a spring-damper system..

3.1 The Linear Solution

If one uses the HBM with linear springs, we expect that the result is identical to the result of a frequency response analysis (in the following denoted as FRF). To this end, we do not use the nonlinear functions of Figure 4 and Figure 5, but only the linear part of the polynomials as depicted in the same figures. The damping is linear with a coefficient of 0.02 [-]. Figure 7 shows the comparison of HBM and FRF, which allows the conclusion that both results are identical as expected.

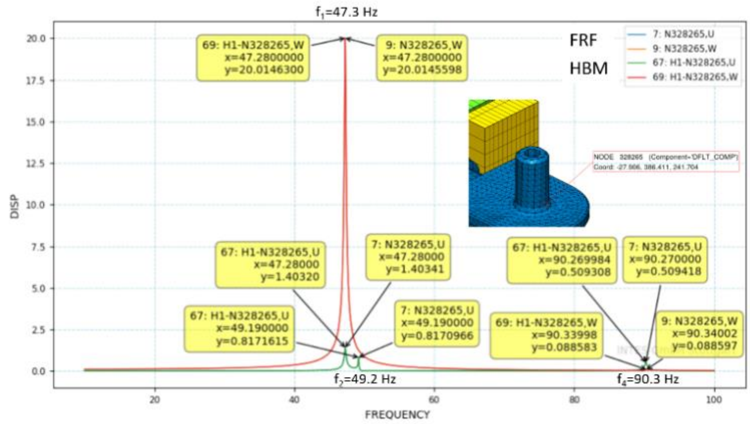

Figure 7. For the reference node 328265, the FRF and HBM displacement results [mm] are shown simultaneously for DOF U and W. The mentioned frequencies [Hz] f1, f2, and f4 are the eigenfrequencies in Z and X direction as well as rotation around the Y axis.

3.2 The Nonlinear Solution

Using the nonlinear functions from Figure 4 and Figure 5 the result is shown in Figure 8 with damping coefficient 0.02. Very typical for nonlinear solutions in frequency domain, one can see multiple solutions for the same frequency. A comparison of linear and nonlinear solution is shown in Figure 9, where the nonlinear solution shows lower peak frequency and higher amplitude. Multiple solutions for one frequency could indicate instabilities. Technical products should avoid instabilities and therefore also multiple solutions. This can be achieved by increasing the damping of the rubber mount. Of course, the used rubber material should be able to provide this higher damping. By increasing the damping coefficient from 0.02 to 0.08, all multiple solutions can be avoided.

Figure 10 shows the comparison of the response curves for both damping coefficients. The response with higher damping coefficient does not show any multiple solutions at same frequency anymore.

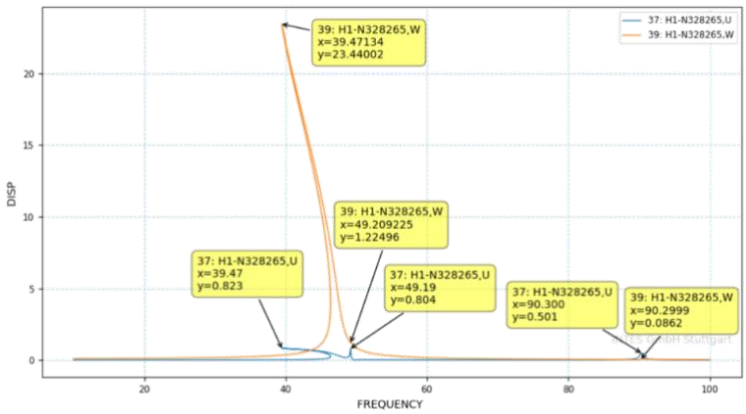

Figure 8. For the reference node 328265, nonlinear HBM displacement results [mm] are shown simultaneously for DOF U and W.

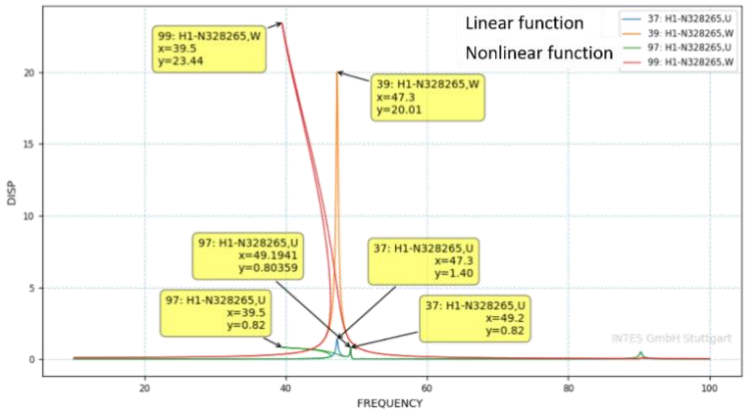

Figure 9. For the reference node 328265, linear and nonlinear HBM displacement results [mm] are shown simultaneously for DOF U and W with same damping coefficient 0.02 [-].

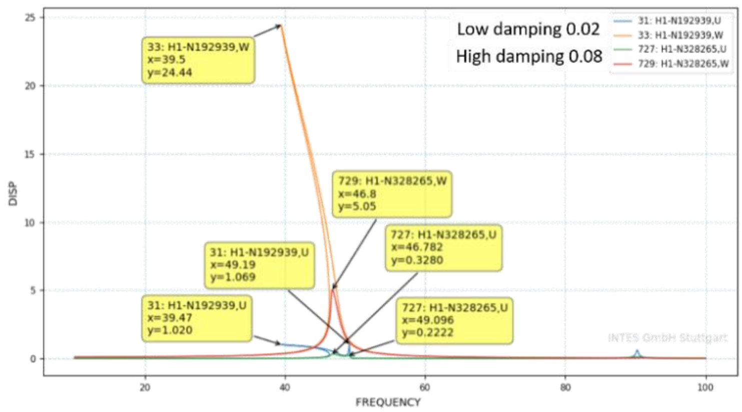

Figure 10. For the reference node 328265, nonlinear HBM displacement results [mm] for damping coefficients 0.02 and 0.08 [-] are shown simultaneously for DOF U and W.

4 Second Analysis: Rubber Mounts with Contact

Our second study will be made with the rubber mounts and contact between pin and rubber mount for each direction. Figure 11 shows the modelling with the rubber mount as in Figure 6 and another nonlinear spring for contact. In addition, a nonlinear spring is added to model the contact. This system has to be duplicated for all directions at all four pins. The three nodes of the spring-damper system and the contact have the same position in space. The node connected to the pin is connected to a center node of the pin, the node between rubber mount and contact is free in one direction, and the end-node of the rubber mount is fixed as in Figure 6.

We expect that the mounting of the radiator is made without any initial gap, so the radiator is not loose but properly fixed in the rubber mounts. Then, all initial gap widths are set to zero. This implies that relative motions between pins and rubber mounts are (almost) not possible. Hence, any frictional damping will not take place. So, additional damping has to come from the rubber mounts only. Figure 12 shows the characteristic of the contact, where the function indicates a linear behaviour in case of a closed contact and no contact force in case of an open contact.

Figure 13 shows the nonlinear response curve when taking contacts into account and with a damping coefficient of 0.08. There are again multiple solutions at some frequencies.

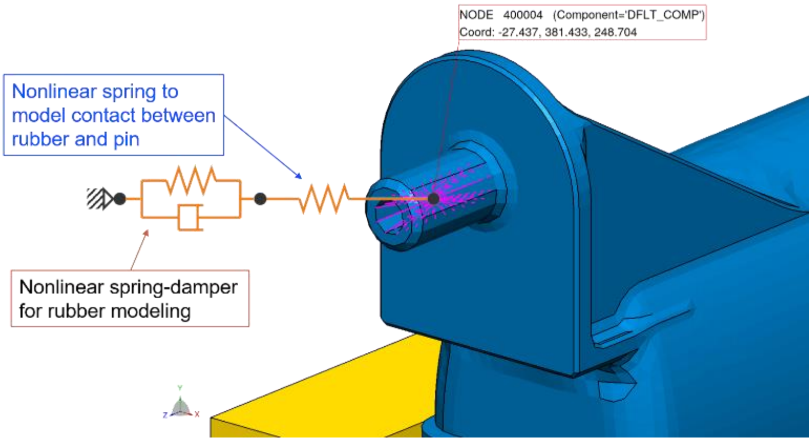

Figure 11. The modeling of a rubber mount by a spring-damper system.

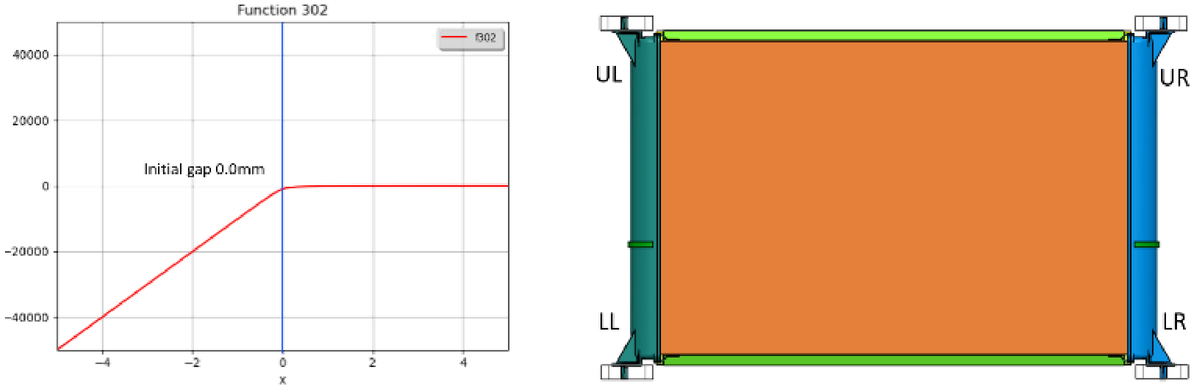

Figure 12. The nonlinear function to model the contact is characterized by a linear behavior in case of a closed contact and no contact force [N] in case on of an open contact.

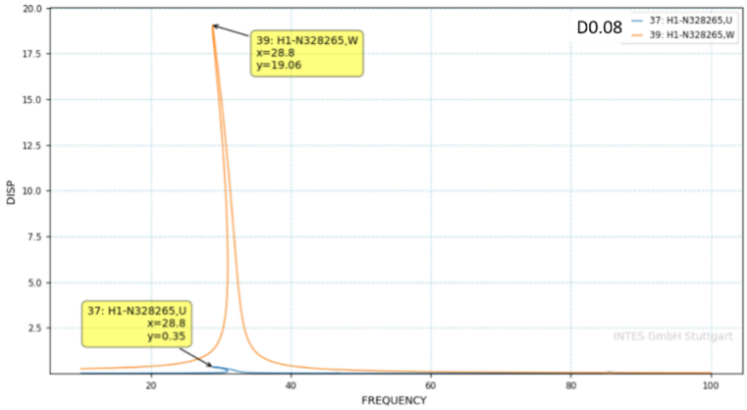

Figure 13. For the reference node 328265, nonlinear HBM displacement results [mm] with rubber mount and contact are shown simultaneously for DOF U and W.

In order to avoid multiple solutions at any frequency the damping coefficient of the rubber mounts has to be increased from 0.08 to 0.2. This is still in the range of possible rubber damping values (≤ 0.3). By increasing the damping coefficient from 0.08 to 0.2, all multiple solutions can be avoided. Figure 14 shows the comparison of the response curves for both damping coefficients. The response with higher damping coefficient does not show any multiple solutions at same frequency anymore.

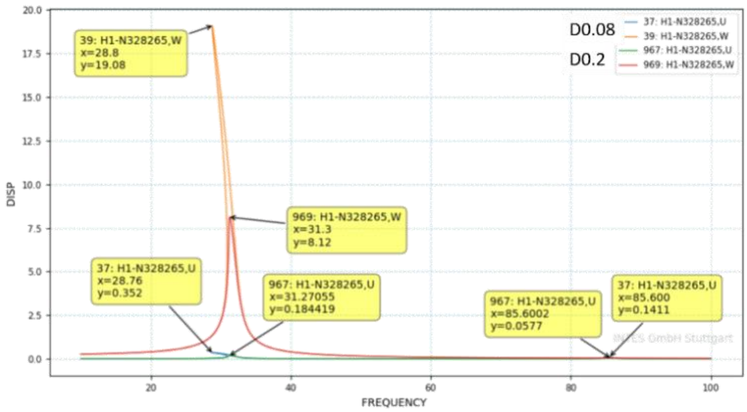

Figure 14. For the reference node 328265, nonlinear HBM displacement results [mm] for damping coefficients 0.08 and 0.2 [-] are shown simultaneously for DOF U and W.

In addition, Figure 15 shows the comparison of the response curves with and without contact, where the damping coefficient is 0.2 for both curves. The main resonance peak is now at 31.3 Hz with contact and at 47.2 Hz without contact. The maximum amplitude is 8 mm with contact and 2 mm without contact. If the mounting cannot avoid contact, the contact case is more critical.

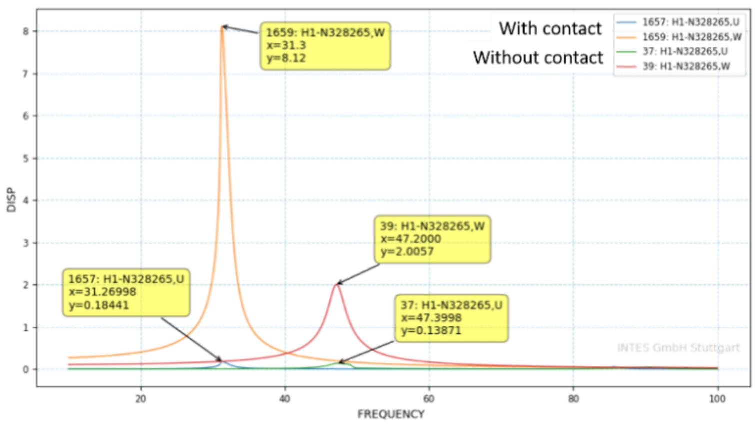

Figure 15. For the reference node 328265, nonlinear HBM displacement results [mm] for damping coefficient 0.2 [-] are shown simultaneously for DOF U and W with and without contact.

5 Transformation to Time Domain

After solving with HBM, we have a solution in frequency domain. Using all calculated harmonics, a transformation to time domain is available. To this end, a frequency out of the HBM analysis is selected together with a timestep and a number of loops.

Taking the frequency of the highest resonance peak at 31.3 Hz (see Figure 15) and using 100 loops, the timestep is

$$\Delta = \frac{1}{100 \cdot 31.3} = 0.0003195\ s$$

With these numbers, one gets two sine wave periods at 31.3 Hz with 200 timesteps. Now, we can check the spring element forces for rubber and contact.

Figure 16 shows the rubber displacement and forces during the vertical motion of the radiator. The effect of contact is clearly visible. If upper contact is closed, the lower contact is open, and vice versa.

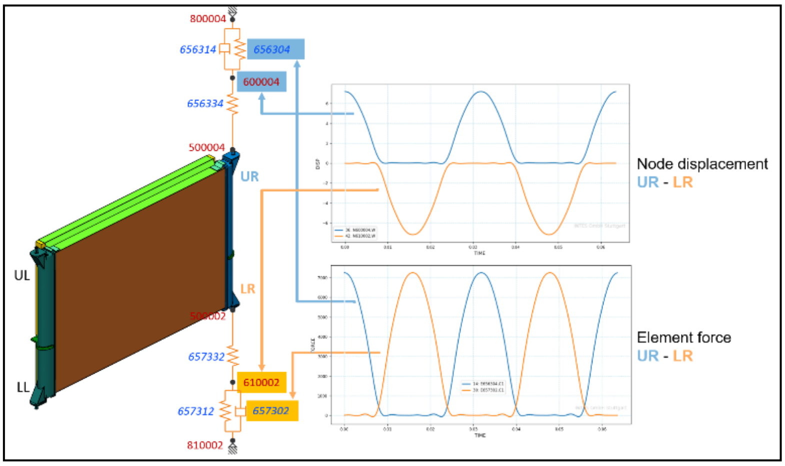

Figure 16. During the vertical vibration of the radiator, the contact at the upper pin is closed while the contact at the lower pin is open and vice versa.

Figure 17 shows the contact displacement [mm] and forces during the vertical motion of the radiator. The input of the contact is freely vibrating, the output shows the typical contact behaviour.

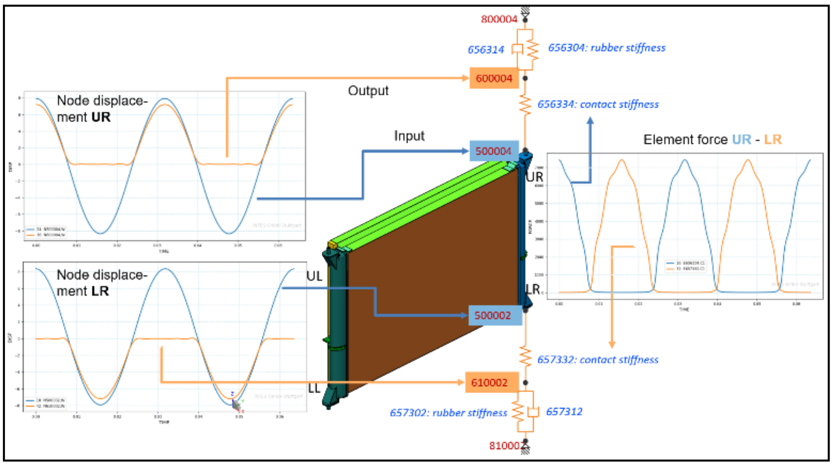

Figure 17. During the vertical vibration of the radiator, the contact input is freely vibrating while the output of the contact cuts any penetration. This behavior is alternating at the upper and lower pin.

6 Fatigue Damage in Frequency Domain

After transformation to time-domain we perform a fatigue damage analysis for a subset of frequencies from 29.9 Hz to 34.9 Hz. Outside this frequency range, the fatigue damage is very close to zero. Then, a fatigue damage is calculated for these frequencies with a timestep of $1/(100 \cdot f)$ and 200 timesteps. Figure 18 shows the SN-curve of the tank material and the fatigue damage distribution over the used frequencies (here with the displacement response at node 357683). Maximum damage and displacement are at 31.36 Hz, 8.1 mm displacement, 1.37E-04 damage. This corresponds to a lifetime of 465 s (2/(dmg**f*)) at this frequency.

In addition, Figure 19 shows the upper part of the right tank with the calculated fatigue damage and the highest damage at 31.36 Hz.

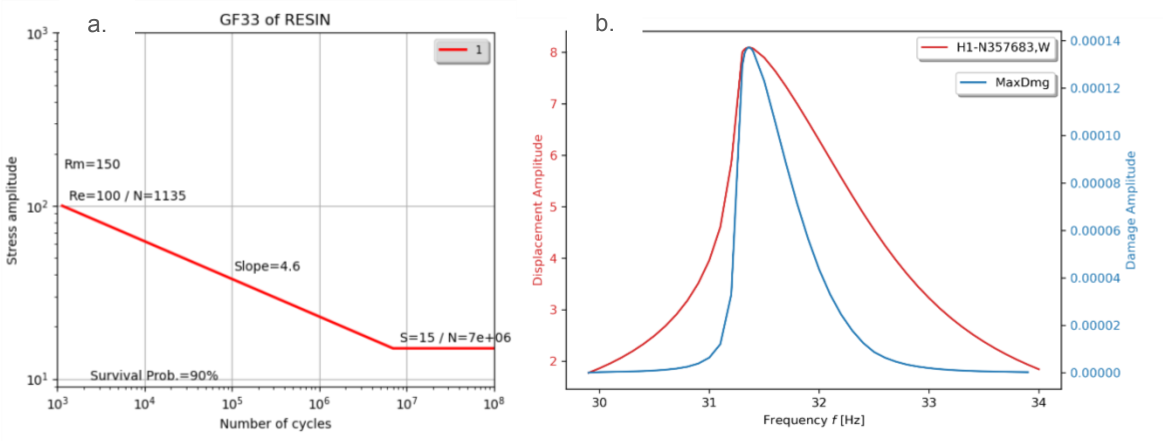

Figure 18.a. SN curve of the tank material, b. the damage [-] is shown over the frequency (in blue) [Hz] and the displacement response (in red) [mm].

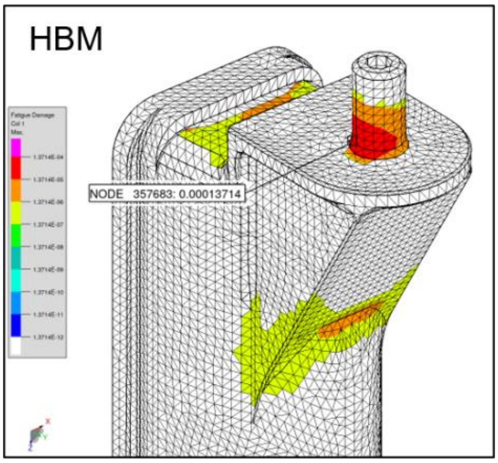

Figure 19. Maximum damage 1.37E-04 at node 357683 for frequency 31.36 Hz.

The remaining point is now to check the maximum damage value by a time-history analysis using the same model with its nonlinear rubber mounts and contacts. A modal time-history analysis with the excitation function at 31.36 Hz is made, because a direct time history delivers the same results but is significantly more computationally intensive. We need the steady-state results avoiding any non-periodic response. Therefore, we take 20000 timesteps and derive the fatigue damage for the last 200 timesteps as for the HBM. Figure 20 shows the time history. Figure 21 shows the fatigue damage in the right upper tank. The difference between HBM and TH (Time-History) result is

$$((TH - HBM))/TH = ((0.00013795 - 0.00013714))/0.00013795 = 0.00587 < 0.6\% .$$

The damage is the same for HBM and time-history analysis, but runtime is much different. The elapsed run time on 28 cores is 1.5 hours for the time-history analysis compared to about 3 minutes with HBM for the same frequency.

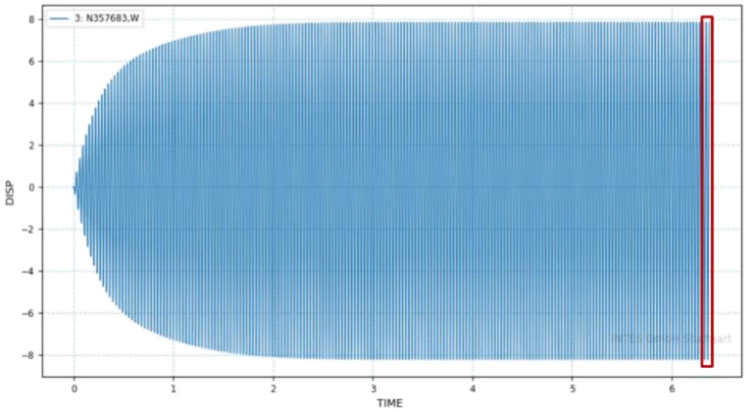

Figure 20. Modal time-history analysis with fatigue damage calculation for the last 200 timesteps (red box).

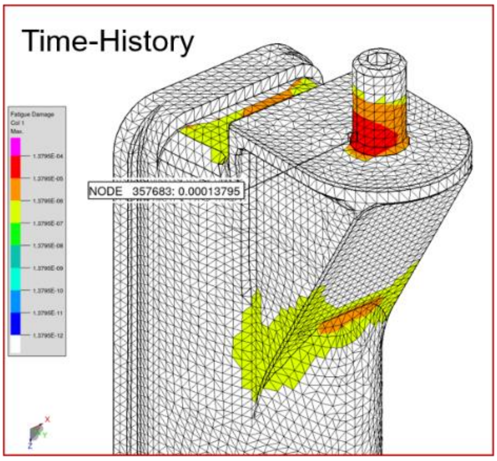

Figure 21. Maximum damage 1.38E-04 from a modal time history analysis at node 357683 for frequency 31.36 Hz.

7 Conclusions

HBM is used to solve nonlinear dynamic problems in frequency domain. Nonlinearities used for the mounting of a radiator-like structure are rubber mounts and contacts at the 4 fixation pins. The force-deflection curve of rubber is made by a separate model but could also come from a test result.

HBM results show multiple solutions for same frequency, which was cured by sufficient damping provided by the rubber mounts in order to avoid instabilities.

HBM results are transformed to time domain and followed by a fatigue analysis providing fatigue damage in frequency domain. For the frequency with the highest fatigue damage, a modal time-history analysis has been made giving the same fatigue damage.

HBM, time-history and fatigue analysis are all integrated in PERMAS, which allows one single job for all three analyses (with a run time of about 3 minutes per frequency).

8 References

[1] Cameron, T.M., Griffin, J.H., “An alternating frequency/time domain method for calculating the steady-state response of nonlinear dynamic systems”, in Journal of Applied Mechanics, Vol. 56, 1989, pp. 149—154, [Online]. Available: https://doi.org/10.1115/1.3176036

[2] Saunders, B.E., Vasconella, R., Kuether, R.J., Abdelkefi, A., “Insights on the continuous representation of piecewise-smooth nonlinear systems: limits of applicability and effectiveness, Nonlinear Dynamics”, [Online]. Available: https://doi.org/10.1007/s11071-021-06436-w

[3] Mahmoodi, A., Ahmadian, H., “Forced Response Vibration Analysis of the Turbine Blade with Coupling between the Normal and Tangential Direction”, Vol. 2022, [Online]. Available: https://doi.org/10.1155/2022/2413022

[4] Lentz, L., von Wagner, U., “Avoidance of artifacts in harmonic balance solutions for nonlinear dynamical systems”, Journal of Theoretical and Applied Mechanics 2020; 58(2): pp. 307–316, [Online]. Available: https://doi.org/10.15632/jtam-pl/118161

[5] Martinelli, C., Coraddu, A. & Cammarano, A., “Approximating piecewise nonlinearities in dynamic systems with sigmoid functions: advantages and limitations”, Nonlinear Dyn 2023, [Online]. Available: https://link.springer.com/article/10.1007/s11071-023-08293-1

[6] PERMAS Examples Manual, INTES Publication No. 550, Stuttgart, 2022.